Journal of
Applied Crystallography

ISSN 0021-8898

Received 23 June 2006
Accepted 14 September 2006

Hyperquenching for protein cryocrystallography

Matthew Warkentin,[a] Viatcheslav Berejnov,[a] Naji S. Husseini[b] and Robert E. Thorne[a]*

[a]Physics Department, Cornell University, Ithaca, NY 14853, USA, and [b]Applied and Engineering Physics Department, Cornell University, Ithaca, NY 14853, USA. Correspondence e-mail: ret6@cornell.edu

When samples having volumes characteristic of protein crystals are plunge cooled in liquid nitrogen or propane, most cooling occurs in the cold gas layer above the liquid. By removing this cold gas layer, cooling rates for small samples and modest plunge velocities are increased to 1.5×10^4 K s^{-1}, with increases of a factor of 100 over current best practice possible with 10 μm samples. Glycerol concentrations required to eliminate water crystallization in protein-free aqueous mixtures drop from ∼28% *w*/*v* to as low as 6% *w*/*v*. These results will allow many crystals to go from crystallization tray to liquid cryogen to X-ray beam without cryoprotectants. By reducing or eliminating the need for cryoprotectants in growth solutions, they may also simplify the search for crystallization conditions and for optimal screens. The results presented here resolve many puzzles, such as why plunge cooling in liquid nitrogen or propane has, until now, not yielded significantly better diffraction quality than gas-stream cooling.

1. Introduction

The introduction of cryocrystallographic methods in the late 1980s revolutionized the determination of protein structures by X-ray diffraction (Hope, 1988, 1990). As is known from cryoelectron microscopy (Zeitler, 1982; Dubochet *et al.*, 1982), lowering the sample's temperature to cryogenic temperatures (∼100 K) dramatically reduces radiation damage. Diffusion of atomic and molecular radicals produced by irradiation is greatly reduced, and the rigidified water network provides a scaffold for the protein that prevents large motions in response to local damage. With advances in synchrotron X-ray sources, optics and X-ray detectors, cryocrystallographic methods now allow complete data sets to be obtained from macromolecular crystals smaller than 10 μm. It is generally assumed (although seldom verified in detail) that a low-temperature structure corresponds to the biologically active form (Frauenfelder *et al.*, 1979; Earnest *et al.*, 1991; Tilton *et al.*, 1992; Young *et al.*, 1994; Kurinov & Harrison, 1995).

Despite these triumphs, cryopreservation of protein crystals has remained a problematic art. Protein crystal order and especially mosaicity nearly always degrade during flash cooling. Many cooled crystals do not yield usable diffraction. Formation of hexagonal ice both inside and outside the crystal can damage it and introduce ice rings that interfere with diffraction from the protein lattice. Ice rings can be eliminated and damage reduced by cooling fast enough to obtain vitreous or amorphous ice. For pure water, the required cooling rates are $\sim 10^6$ K s^{-1} (Bruggeller & Mayer, 1980; Johari *et al.*, 1987), orders of magnitude larger than those achieved in current cryocrystallography practice. Adding cryoprotectants such as glycerol, ethylene glycol and MPD can reduce required cooling rates to 10^2 K s^{-1} or less (Peyridieu *et al.*, 1996; Lu & Liu, 2003). Unfortunately, cryoprotectants can be unfriendly to the protein's native conformation, they can cause osmotic stress, and they affect protein solubility, and so can cause crystal cracking, dissolution and structural changes, especially at the relatively high concentrations (20–30% *w*/*v*) used in current practice. Furthermore, internal solvent (the crystallization of which is strongly inhibited by the protein) and external solvent should in general be cryoprotected differently (Kriminski *et al.*, 2002). As a result, optimizing cryoprotectant conditions can be time consuming.

Protein crystals are cooled by direct insertion into a stream of cold nitrogen gas at $T \simeq 100$ K, or by plunging into liquid nitrogen ($T_v = 77$ K) or liquid propane ($T_m = 86$ K) (Rodgers, 1994; Chayen *et al.*, 1996; Garman & Schneider, 1997; Garman, 1999; Pflugrath, 2004; Juers & Matthews, 2004). Simple physical arguments, scaling analysis (Kriminski *et al.*, 2003) and the experience of cryoelectron microscopists clearly suggest that plunge cooling in liquid cryogens should produce far larger cooling rates and thus better (or at least different) diffraction outcomes than gas-stream cooling. However, diffraction outcomes obtained using cold gases and liquids have not differed substantially, and two studies to determine the most effective method (Teng & Moffat, 1998; Walker *et al.*, 1998) reached different conclusions, so that both methods remain in wide use (Garman & Owen, 2006). Even more puzzling, and troubling, is that the measured cooling rates achieved in conventional plunge or gas-stream cooling of ordinary-size samples (200–1500 K s^{-1}) are small (Teng & Moffat, 1998; Walker *et al.*, 1998; Snell *et al.*, 2002). Crystals

take a fraction of a second to cool below the solvent's glass transition temperature T_g [136 K for pure water (Johari *et al.*, 1990; Johari, 2005), ~150 K for 30% glycerol solutions (*e.g.* Harran, 1978; Chinte *et al.*, 2005) and perhaps higher for internal crystal solvent in small channels (Weik *et al.*, 2001, 2004, 2005)] and of the order of 0.1 s to cool below $T = 220$ K, where conformational motions are largely frozen out (Frauenfelder *et al.*, 1979; Tilton *et al.*, 1992; Halle, 2004).

Here we show that during plunge cooling into liquid cryogens of the small volume (<0.1 µl) samples typical in protein crystallography, the cooling rate in the critical region between room temperature and $T = 150$ K is controlled not by the liquid but by heat transfer to the cold gas layer that exists above it. By removing this cold gas layer, cooling rates can be increased to at least 1.5×10^4 K s^{-1} in liquid nitrogen and cooling times to $T = 100$ K reduced to < 10 ms. With these high cooling rates, cryoprotectant concentrations required to achieve vitrification of water–glycerol mixtures are reduced from ~30% to less than 6% *w*/*v*. Consequently, cooling-induced crystal damage should be reduced, and cryoprotectant screening should be simplified.

2. Methods and results

2.1. Plunge cooling of small volumes: a puzzle

To obtain vitreous ice, the time to cool to below T_g should be shorter than the characteristic time for nucleation of crystalline ice. Cryoprotectants like glycerol slow or inhibit crystalline ice nucleation, decreasing the required cooling rate. Smaller volume samples have larger surface-to-volume ratios and should cool more quickly, decreasing the required cryoprotectant concentration. An elementary analysis suggests that the cooling rate should scale as $V^{-1/2}$ (Kriminski *et al.*, 2003).

Berejnov *et al.* (2006) examined the minimum concentration required to achieve vitrification of aqueous mixtures of 14 different cryoprotectants as a function of the liquid volume V, for plunge cooling in liquid nitrogen using standard methods. As illustrated in Fig. 1 (open circles) for glycerol, at large volumes (> 10 µl) Berejnov *et al.* found that the required cryoprotectant concentration is large and independent of volume, as expected in the limit when cooling rates are so slow that nucleation must be completely inhibited. At smaller volumes, the cryoprotectant concentration decreases with decreasing volume, as expected based on the argument in the preceding paragraph. However, for volumes below ~0.1 µl (for glycerol and all other cryoprotectants studied by Berejnov *et al.*) the required cryoprotectant concentration becomes roughly independent of volume. Similar volume-independent glycerol concentrations were required for volumes below ~0.1 µl when drops were plunge cooled in liquid propane. This volume range corresponds to crystals smaller than about 500 µm in all three dimensions, *i.e.* to essentially all crystals of interest in macromolecular X-ray crystallography.

The apparent small-volume saturation found by Berejnov *et al.* cannot represent an intrinsic feature of glycerol–water mixtures because pure water can be vitrified at high cooling rates (Mayer, 1985). To explore the origin of this saturation, aqueous mixtures were prepared in 2% *w*/*v* glycerol increments. An aerosol spray of each mixture deposited drops with a range of sizes onto the bottom of a cup made from 25 µm copper foil. The cup plus drops was then plunged into liquid nitrogen and the result photographed through a microscope. As in previous work (Garman & Schneider, 1997; McFerrin & Snell, 2002; Chinte *et al.*, 2005; Berejnov *et al.*, 2006), clear drops were judged to be vitrified, while opaque drops were judged to be polycrystalline. The largest drop volume for which the drops were consistently transparent was then recorded as the critical volume for vitrification at that glycerol concentration. Drop volumes were estimated based on the drop radius and separate calibration measurements of drop height *versus* radius on copper foil.

Copper's thermal conductivity is much larger than that of the boiling gas layer that envelops drops when they are directly plunged into liquid cryogens. This fact is used to advantage in the splat freezing method (in which drops are sprayed onto cold metals) to vitrify ~10 µm drops of pure water (Mayer, 1985). Our variant of this method yields frozen drops with much simpler shapes, allowing more accurate volume estimation. As shown by the solid circles in Fig. 1, the saturation of critical concentration at small drop volumes disappears, and the concentration decreases monotonically (approximately logarithmically) with volume down to the smallest volume (~40 pl) studied. The saturation of concentration observed by Berejnov *et al.* in plunge cooling of volumes below 0.1 µl must then result because the cooling rate becomes roughly independent of volume. Consequently, with

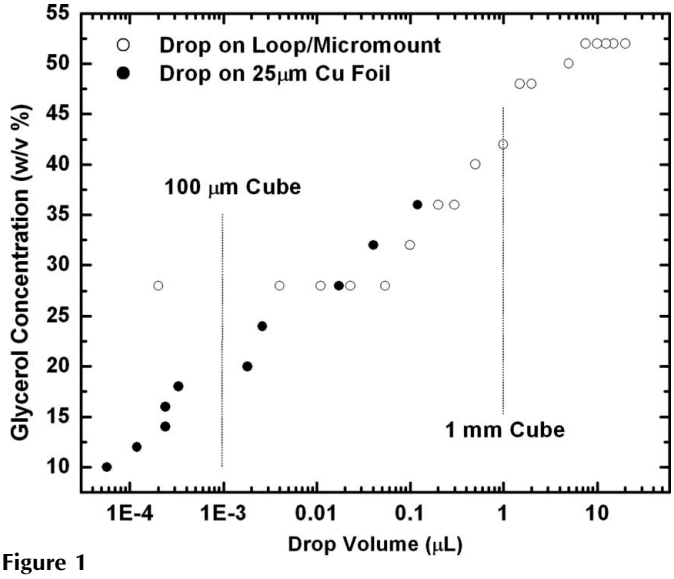

Figure 1
Minimum glycerol concentration required for vitrification of glycerol–water mixtures *versus* drop volume. Open circles are data collected by plunging drops held in tungsten wire loops (for volumes above 1 µl) or in MicroMounts (below 1 µl) into liquid nitrogen without removing the cold gas layer [from Berejnov *et al.* (2006)]. Solid circles represent data collected by spraying drops onto the bottom of a 25 µm thick copper cup and then plunging into liquid nitrogen. Vertical lines indicate corresponding linear dimensions of cubic samples.

current methods smaller protein crystals do not cool appreciably faster than large ones. This explains in part why cryoprotectant conditions required to cool small crystals are found to be similar to those for large ones.

2.2. The cold gas layer: temperature *versus* height above the liquid cryogen

The gas immediately above a liquid cryogen will be cooled through radiation, convection and conduction by the cold liquid below. For large sample volumes, the sample can pass through the resulting cold gas layer without appreciable internal temperature drop, so that cooling occurs mainly in the liquid cryogen. For small sample volumes, the sample will remain in equilibrium with the surrounding gas as it passes through the cold gas layer. Most of the cooling, as well as solidification of the solvent within the sample (vitrification or crystallization), may then occur in the gas, before the sample reaches the liquid. The dangers of cold gas layers have been discussed in the context of cryoelectron microscopy (Ryan *et al.*, 1992), and the problem of heat transfer from a small drop moving through the cold gas above a liquid cryogen has been analyzed (Chang & Baust, 1991). In the protein crystallography community, the cold gas layer's existence has been recognized (Pflugrath, 2004) but its effects have not been quantified.

To quantify the cold gas layer, a glass hemispherical Dewar, 12 cm across and 8 cm deep (Pope Scientific Inc, Saukville, WI, USA), was filled with liquid nitrogen at T = 77 K. The temperature of the gas above the liquid was measured using a chromel–constantan (E-type) bare-wire thermocouple with a 120 µm bead and 75 µm diameter leads, and recorded using a computer with an SCB-386 DAQ interface and running *LabView* (http://www.ni.com/labview/). The thermocouple was initially positioned well above the liquid nitrogen surface and then lowered by a stepper motor under computer control. The recorded temperature *versus* time was converted to temperature *versus* height using the measured speed of the stepper motor. To check for *e.g.* radiative cooling of the thermocouple below the gas temperature, measurements were repeated at speeds from 0.1 to 5 mm s^{-1} and in the reverse direction, and no appreciable variation in temperature profiles was observed. To emulate conditions used by crystallographers, no special effort was made to isolate the Dewar, and so air currents in the room chaotically perturbed the gas layer. Measurements were thus repeated until a satisfactorily clean curve was obtained. Temperature *versus* height profiles were recorded at different radial distances from the Dewar's center, and showed no measurable variations from the center to the inner walls.

Fig. 2 shows the resulting temperature profiles obtained when the Dewar was filled to its brim and to levels 2 and 4 cm below its brim. With the Dewar filled to the brim, the gas temperature falls below water's freezing point 1 cm above the surface, and below water's glass transition T_g about 4 mm above the surface. For a more typical and safe fill level of 4 cm, the cold gas layer extends more than 2 cm above the liquid surface, and the temperature drops below T_g nearly 1 cm above the liquid surface.

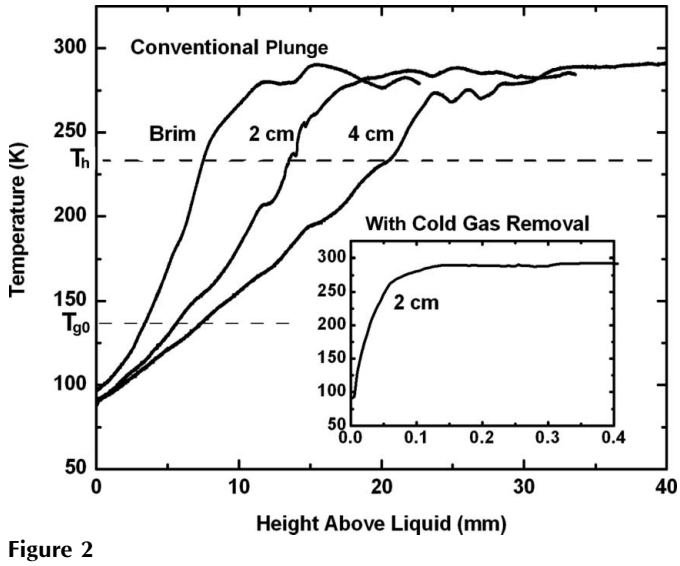

Figure 2
Gas temperature as a function of height above liquid nitrogen, held in a 12 cm diameter hemispherical Dewar, for different liquid fill levels (measured in cm from the brim). Fluctuations at large height are due to room air currents. Inset: gas temperature *versus* height above liquid nitrogen when dry nitrogen gas is blown along the thermocouple's path, as described in the text. Blowing reduces the thickness of the cold gas layer above the liquid from ~2 cm to less than 100 µm: a reduction of more than two orders of magnitude. T_h and T_{g0} denote pure water's homogeneous nucleation temperature and glass transition temperature, respectively.

2.3. Plunging through cold gas

We next investigated cooling rates obtained when plunging a thermocouple through the cold gas layer into liquid nitrogen, as a function of the layer thickness (Dewar fill level) and plunge velocity. To obtain the fastest temperature response time, a thermocouple with an 80 µm bead and 25 µm diameter leads was flattened between two machine-tool bits to a thickness of 20 µm. This allowed us to explore the thermal mass/response time regime relevant to cryocooling sub-100 µm protein crystals. Our geometry is particularly relevant to crystals with thin plate or rod-like morphologies. The thermocouple was plunged by hand, and the plunge velocity was determined using frame-by-frame analysis of a video of the experiment.

Fig. 3 shows the temperature of the thermocouple during plunges into liquid nitrogen at different plunge velocities. In Fig. 3(*a*), the Dewar was filled to 4 cm from its brim, and in Fig. 3(*b*) it was filled to the brim. Arrows on each curve indicate the point at which the thermocouple entered the liquid nitrogen. For all conditions studied, the thermocouple cools within the gas layer below water's freezing point, and below water's homogeneous nucleation temperature (233 K) for all but the fastest plunge into a full Dewar. For conditions most closely matching those used in typical cryocrystallography practice (a Dewar filled 4 cm below the brim and a plunge speed of 0.4 m s^{-1}) the thermocouple cools below T_g within the gas layer. The time required is ~0.1 s, corresponding to a

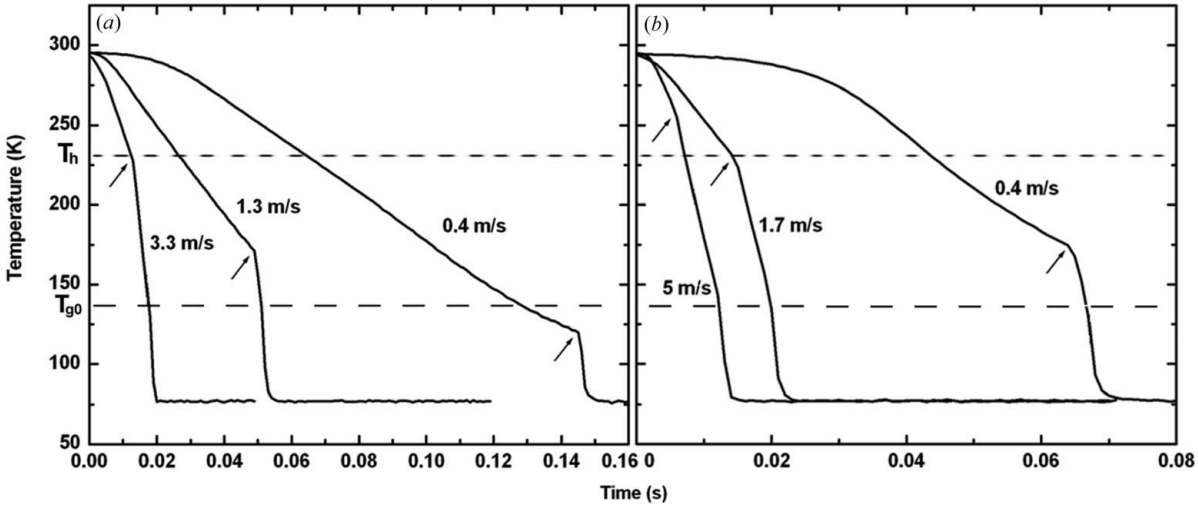

Figure 3
Temperature *versus* time recorded as a thermocouple is plunged at different velocities into a Dewar of liquid nitrogen. The liquid level is (*a*) 4 cm from the brim and (*b*) at the brim. Arrows indicate the time when the thermocouple enters the liquid. Measurements used a chromel–constantan bare-wire thermocouple with 25 µm leads and a flattened, ∼20 µm thick, bead (see text). T_h and T_{g0} denote pure water's homogeneous nucleation temperature and glass transition temperature, respectively.

cooling rate of 1500 K s^{-1}. This is only three times larger than reported by Teng & Moffat (1998), despite our use of a thermocouple six times thinner and with leads six times smaller in diameter.

The maximum cooling rate prior to entering the liquid increases roughly linearly with increasing plunge velocity. Once the thermocouple enters the liquid, the cooling rate in all cases is much larger (∼15000 K s^{-1}). Unlike in the gas, cooling rates in liquid are largely unaffected by the plunge velocity in the velocity range examined.

One way to defeat the cold gas layer is to plunge at high velocity (>5 m s^{-1}) into a full Dewar. High-speed plunging is used in commercial devices for cooling electron microscopy samples, which consist of very thin (sub-micrometre) films mounted on thick (20–30 µm) metal grids that have much higher thermal mass than protein crystallography mounts. It is not clear that the more delicate samples and mounts used in protein crystallography could routinely survive such treatment, except when the sample thickness and thus the force on entering the liquid is small. Large accelerations and decelerations (> 100 times that due to gravity), required for a compact device and to prevent enormous splashing when the goniometer base holding the sample impacts the liquid cryogen, could also be problematic.

2.4. Removing the cold gas layer

Another way to increase cooling rates is to remove the cold gas layer, producing an abrupt transition along the plunge path from gas at room temperature to liquid at cryogenic temperature. To remove the cold gas layer, we simply blow it away.

A Teflon nozzle with a diameter of 8 mm was connected to a cylinder of dry nitrogen gas through a high flow-rate rotameter. The nozzle was positioned 30 cm from the liquid level and tipped 10° from the vertical, and its flow directed at the radial center of the liquid surface. Other geometries for the nozzle and its positioning were examined and most were found to be satisfactory, but the geometry described here gave the most repeatable results.

The inset to Fig. 2 shows the dramatic effect of blowing on the temperature profile. Nitrogen gas flowing at 20 l min^{-1}, corresponding to a maximum velocity at the nozzle of ∼6.6 m s^{-1}, was directed at the liquid nitrogen surface in a Dewar filled to within 2 cm of its brim. The temperature falls below water's melting point at a height of ∼80 µm above the liquid surface, and below water's glass transition at ∼20 µm, a height comparable to the thickness of the thermocouple bead used to measure the profile. Our simple blowing procedure thus reduces the gas layer thickness by a factor of at least 300. At a modest plunge velocity of 0.4 m s^{-1}, the time to traverse this layer is less than 0.2 ms, more than 500 times shorter than the cooling times without gas layer removal in Fig. 3. Consequently, nearly all the cooling during a plunge should occur in the liquid, not the gas.

2.5. Cooling rates with cold gas layer removal

To test the effect of cold gas layer removal on cooling rates, samples were plunged in the presence of flowing nitrogen gas. The gas flow was turned on prior to the plunge and then turned off just after the sample was beneath the liquid surface so as to minimize nitrogen boil-off. (For liquid propane and ethane, flowing gas can warm the liquid layers near the surface above T_g, so minimizing the time the gas is on is even more important.) Fig. 4 shows the resulting temperature profile obtained with a 20 l min^{-1} gas flow when the thermocouple was plunged at 0.3 m s^{-1} along the axis of a Dewar filled to within 2 cm of its brim. Unlike in all of the data of Fig. 3, there is no evidence of cooling by the gas; all cooling occurs in the liquid nitrogen. The cooling time from room temperature to below T_g is ∼0.01 s, ten times shorter than without gas

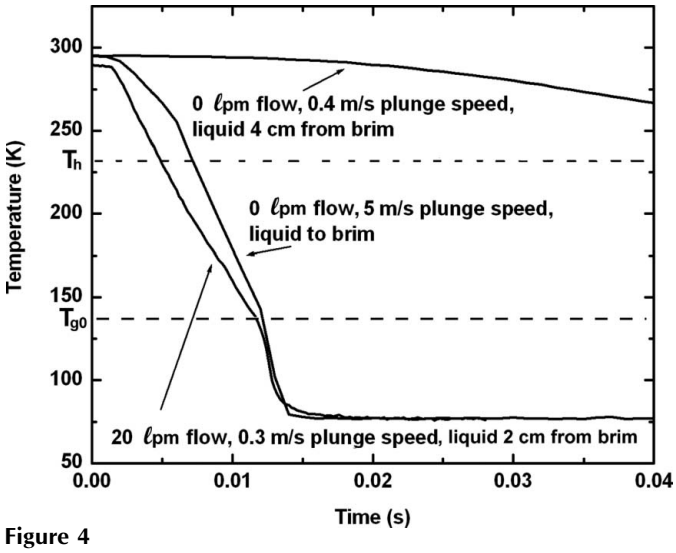

Figure 4
Temperature *versus* time recorded as a thermocouple is plunged into liquid nitrogen, with and without cold gas layer removal by blowing. Without blowing, the plunge velocity required to minimize the effect of the gas layer is $\sim$5 m s^{-1}. With blowing, very similar curves are obtained for all plunge velocities and fill heights. These measurements used the same thermocouple as in Fig. 3. T_h and T_{g0} denote pure water's homogeneous nucleation temperature and glass transition temperature, respectively.

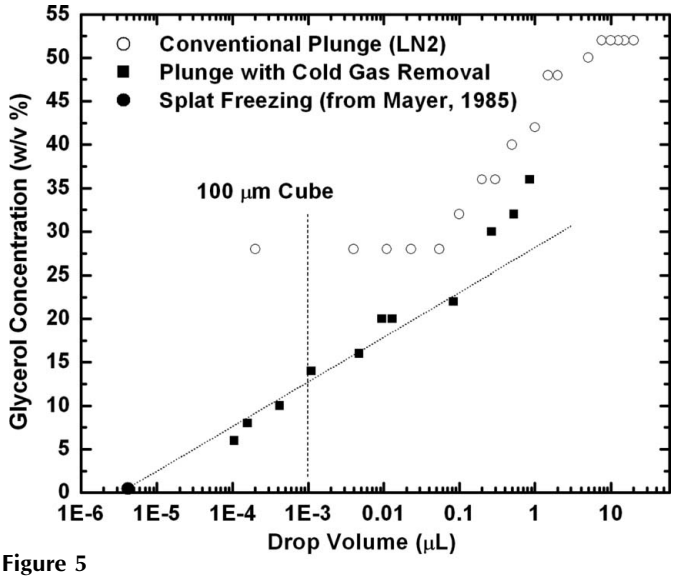

Figure 5
Minimum glycerol concentration required for vitrification of glycerol–water mixtures *versus* drop volume. Open circles are the data of Fig. 1 for a direct plunge into liquid nitrogen without cold gas layer removal, taken from Berejnov *et al.* (2006). Solid squares are data collected for a direct plunge into liquid nitrogen using a dry nitrogen gas stream to remove the cold gas layer. These data show an approximate logarithmic variation of concentration with volume over four orders of magnitude in volume (suggesting an exponential variation of critical cooling rate with concentration). Extrapolating this variation to zero concentration roughly yields the maximum volume of pure water that can be vitrified by spraying drops onto cold copper surfaces.

removal. The average cooling rate over this temperature range is 15000 K s^{-1}, ten times larger, and slightly larger than the cooling rate achieved without gas removal at a plunge velocity of 5 m s^{-1} into a full Dewar. Very similar temperature–time curves are obtained for plunge velocities from 0.01 to 1 m s^{-1} and flow rates from 10 to 60 l min^{-1}, with only a slight increase in liquid cooling rate for larger plunge velocities. This is a significant advantage of cold gas layer removal: very large cooling rates are achieved even with very leisurely plunges that pose no risk to the sample.

In every temperature history shown in Figs. 3 and 4 in which the thermocouple enters the liquid with a temperature well above 150 K (*i.e.* with blowing or high plunge velocities), there is a transition to a higher cooling rate at 130–150 K. This is due to a change from film boiling to nucleate boiling of the nitrogen near the sample surface (Incropera & DeWitt, 2002). In the film boiling regime, the cooling rate within the liquid increases slightly with increasing plunge velocity (roughly 30% for a factor 15 in velocity). A similar very weak dependence of cooling rate on plunge velocity is observed in liquid propane and ethane, which cool only in the nucleate boiling regime (Ryan *et al.*, 1992).

2.6. Tiny cryoprotectant concentrations for tiny samples

Finally, we return to the experiments of Berejnov *et al.* (2006) on the minimum (critical) cryoprotectant concentration required to achieve vitreous ice as a function of sample volume. Glycerol–water drops mounted on MicroMounts (Mitegen, Ithaca, NY) and ranging in size from 1 μl to 100 pl were plunge cooled into liquid nitrogen, using the setup described in §2.4 to remove the cold gas layer. The state of the drop (vitreous or polycrystalline) after plunge cooling was deduced by visual observation through a microscope, as described by Berejnov *et al.* The results are shown in Fig. 5, along with those of Berejnov *et al.* obtained without cold gas removal. The small-volume saturation of critical concentration is removed, and glycerol concentrations decrease monotonically with drop volume down to the smallest drop examined. At all volumes studied, the required concentrations are somewhat lower than for drops cooled on copper foil (Fig. 1). For a 100 pl drop, corresponding to a 60 μm diameter sample, the required glycerol concentration is reduced from 28% *w*/*v* without blowing to 6% *w*/*v*. The point for vitrification of pure water (0% glycerol) at a volume of $\sim$4 pl was measured by Mayer (1985) using splat freezing on cold copper. If the extrapolation of the fit to our data in Fig. 5 is valid, then plunging into liquid nitrogen with cold gas removal should cool small samples as effectively as splat freezing, the standard method for achieving the highest cooling rates.

3. Discussion

3.1. Two limiting approaches to cryopreservation

One can imagine two limiting approaches to cryopreservation. The first is to cool very slowly (*e.g.* 0.1 K s^{-1}), using large cryoprotectant concentrations (*e.g.* 60% *w*/*v* glycerol) or high pressures (Kim *et al.*, 2005, 2006) to prevent crystallization. Since all physico-chemical properties are temperature dependent, this might allow relaxations and redistributions to occur so as to maintain quasi-equilibrium and achieve a

homogeneous low-temperature state. Slow cooling with large cryoprotectant concentrations has been used for cryopreservation of cells and tissues (Mazur, 1970), but in most cases this approach is impractical for protein crystals.

The other limiting approach is to cool so quickly that the high-temperature state is frozen in. This approach is loosely referred to as hyperquenching, and is typically achieved by splat cooling on cold metals (Mayer, 1985; Johari *et al.*, 1987).

Unfortunately, current approaches to cryopreservation of protein crystals by plunge or gas-stream cooling give intermediate cooling rates of 10^2–10^3 K s^{-1} (Teng & Moffat, 1998; Walker *et al.*, 1998), and thus are not in either favorable limit. Although sufficiently fast to produce full solvent vitrification (with sufficient cryoprotectant), these modest cooling rates produce inhomogeneities within the crystal (evident in X-ray topography and in measurements of lattice constant distributions) that correlate with degradation of mosaicity and resolution (Kriminski *et al.*, 2002). These inhomogeneities are due at least in part to incomplete relaxation of stresses associated with differential thermal expansion of solvent and protein that can occur at modest cooling rates (Juers & Matthews, 2001; Kriminski *et al.*, 2002). Most conformational flexibility is thought to be frozen out by T = 220 K, but with current methods the time to cool to this temperature can be of the order of 0.1 s. This is sufficiently long to allow side chains (perhaps including those in the active site of a protein) to undergo important conformational changes (Deacon *et al.*, 1997; Scheidig *et al.*, 1999; Sandalova *et al.*, 1999).

3.2. Cold gas layer removal as a route to hyperquenching

Our experiments show that cooling rates of protein crystals can be increased by at least a factor of 10–20 over current best practice, to greater than 15000 K s^{-1} in liquid nitrogen, by removing the cold gas layer above the liquid. The cooling rate should vary roughly as the square root of crystal volume [consistent with the data in Fig. 5 and a more detailed analysis by Berejnov *et al.* (2006)]. Using ∼10 µm microcrystals and liquid propane or ethane, cooling rates approaching 100000 K s^{-1} should be achievable. The apparatus required to achieve these large improvements over current practice is trivial.

Flowing dry gas can dehydrate crystals, especially very small crystals, very quickly. Since the cold gas layer is only ∼2 cm thick, the experimental geometry can be adjusted to confine the flowing gas to this thickness. At a modest plunge velocity of 0.3 m s^{-1}, a crystal will traverse the dry gas in less than 0.1 s. For the smallest crystals, dehydration can be further reduced by reducing the gas flow immediately prior to the plunge.

3.3. Puzzles resolved

The presence of the cold gas layer explains the saturation of minimum cryoprotectant concentrations required to achieve vitreous ice at volumes below ∼0.1 µl, observed for plunge cooling in both liquid nitrogen and liquid propane (Berejnov *et al.*, 2006). For essentially the entire range of sample sizes of relevance in protein crystallography and for experimentally convenient plunge velocities, much of the cooling occurs in the cold gas layer, not the liquid. The fact that the cryoprotectant concentration is roughly volume independent (rather than just showing a change in slope) for volumes below 0.1 µl suggests that these volumes remain in quasi-equilibrium with the surrounding gas during the plunge. For the same plunge velocity and cold gas layer thickness, they all then cool at the same rate, and so require the same cryoprotectant concentration.

Cooling in the cold gas layer may in part explain why flash-cooling outcomes for samples prepared and cooled in seemingly similar ways can be so variable. The one good crystal obtained may have been plunged as a laboratory colleague walked by, blowing away the cold gas.

Cooling in the cold gas layer explains why plunge cooling in liquid cryogens has so far not proven to be reliably superior to cooling in cold gas streams. In all cases, cooling rates have been limited by heat transfer to a gas, not to a liquid.

Cooling in the cold gas layer also provides an additional explanation for why cooling crystals in large blobs of solvent or oil sometimes improves diffraction quality (Gakhar & Wiencek, 2005). By increasing the thermal mass of the sample, little cooling occurs within the cold gas layer, so that the temperature drops from 273 K to below 150 K in the liquid, not the gas. The cooling rate through this important temperature range is decreased because the surrounding liquid decreases the sample's surface-to-volume ratio, but is increased by a factor of ten or more because heat transfer occurs in the liquid, not the gas above it. Consequently, in some size range larger samples should actually cool faster than smaller ones. With cold gas layer removal, cooling rates will be maximized by minimizing surrounding liquid and sample volume.

3.4. Implications for macromolecular crystallography

The present results, by allowing implementation of highly reproducible cooling protocols with dramatically increased cooling rates, will have broad consequences for macromolecular crystallography. Increased cooling rates may reduce conformational changes between room- and low-temperature structures. They will reduce the relaxations that occur during slow cooling and that give rise to inhomogeneities responsible for mosaic broadening and resolution degradation. They will dramatically reduce, by a factor of four or five, the cryoprotectant concentrations required to prevent formation of crystalline ice in protein-free solution that may surround the crystal, simplifying the search for cryoprotection conditions. Furthermore, because the high protein concentrations within the crystal provide excellent protection against ice crystallization (Kriminski *et al.*, 2002), it may routinely be possible to go from crystallization tray to liquid cryogen to X-ray beam and obtain usable diffraction with no cryoprotectants, for all but the highest-solvent-content crystals. Cryoprotectants play other roles aside from inhibiting ice crystallization (Juers & Matthews, 2001; Kriminski *et al.*, 2002), and so they may still be required to obtain the best resolution.

4. Conclusion

Cooling protein crystals by plunging into liquid cryogens has been powerfully enabling and annoyingly troublesome, dramatically reducing radiation damage while introducing other damage that limits the quality of X-ray determined structures. It has long been evident that there is a cold gas layer above the liquid cryogen, and that this gas layer can cool a sample that passes through it. What has not been evident is that, for sample sizes spanning essentially the entire range of interest in protein crystallography, most cooling occurs in this gas layer, not in the liquid cryogen. This unfortunate coincidence has limited cooling rates, allowing internal relaxations that disrupt crystal order. By banishing the cold gas layer, the full potential of plunge cooling to capture and preserve protein structure may finally be realized.

This work was funded by the National Institutes of Health (R01 GM65981).

References

Berejnov, V., Husseini, N. S., Alsaied, O. A. & Thorne, R. E. (2006). *J. Appl. Cryst.* **39**, 244–251.
Bruggeller, P. & Mayer, E. (1980). *Nature (London)*, **288**, 569–571.
Chang, Z. H. & Baust, J. G. (1991). *J. Microsc.* **161**, 435–444.
Chayen, N. E., Boggon, T. J., Cassetta, A., Deacon, A., Gleichmann, T., Habash, J., Harrop, S. J., Helliwell, J. R., Nieh, Y. P., Peterson, M. R., Raftery, J., Snell, E. H., Hadener, A., Niemann, A. C., Siddons, D. P., Stojanoff, V., Thompson, A. W., Ursby, T. & Wulff, M. (1996). *Q. Rev. Biophys.* **29**, 227–278.
Chinte, U., Shah, B., DeWitt, K., Kirschbaum, K., Pinkerton, A. A. & Schall, C. (2005). *J. Appl. Cryst.* **38**, 412–419.
Deacon, A., Gleichmann, T., Kalb, A. J., Price, H., Raftery, J., Bradbrook, G., Yariv, J. & Helliwell, J. R. (1997). *J. Chem. Soc. Faraday Trans.* **93**, 4305–4312.
Dubochet, J., Lepault, J., Freeman, R., Berriman, J. A. & Homo, J. C. (1982). *J. Microsc.* **128**, 219–237.
Earnest, T, Fauman, E., Craik, C. S. & Stroud, R. (1991). *Proteins Struct. Func. Genetics*, **10**, 171–187.
Frauenfelder, H., Petsko, G. A. & Tsernoglou, D. (1979). *Nature (London)*, **280**, 558–563.
Gakhar, L. & Wiencek, J. M. (2005). *J. Appl. Cryst.* **38**, 945–950.
Garman, E. (1999). *Acta Cryst.* D**55**, 1641–1653.
Garman, E. F. & Owen, R. L. (2006). *Acta Cryst.* D**62**, 32–47.
Garman, E. F. & Schneider, T. R. (1997). *J. Appl. Cryst.* **30**, 211–237.
Halle, B. (2004). *Proc. Natl Acad. Sci. USA*, **101**, 4793–4798.
Harran, D. (1978). *Bull. Soc. Chim. Fr. Part. I*, pp. I40–I44.
Hope, H. (1988). *Acta Cryst.* B**44**, 22–26.
Hope, H. (1990). *Annu. Rev. Biophys. Biophys. Chem.* **19**, 107–126.
Incropera, F. P. & DeWitt, D. P. (2002). *Fundamentals of Heat and Mass Transfer*, 5th ed. New York: J. Wiley.
Johari, G. P. (2005). *Phys. Chem. Chem. Phys.* **7**, 1091–1095.
Johari, G. P., Hallbrucker, A. & Mayer, E. (1987). *Nature (London)*, **330**, 552–553.
Johari, G. P., Hallbrucker, A. & Mayer, E. (1990). *J. Chem. Phys.* **92**, 6742–6746.
Juers, D. H. & Matthews, B. W. (2001). *J. Mol. Biol.* **311**, 851–862.
Juers, D. H. & Matthews, B. W. (2004). *Q. Rev. Biophys.* **37**, 105–119.
Kim, C. U., Hao, Q. & Gruner, S. M. (2006). *Acta Cryst.* D**62**, 687–694.
Kim, C. U., Kapfer, R. & Gruner, S. M. (2005). *Acta Cryst.* D**61**, 881–890.
Kriminski, S., Caylor, C. L., Nonato, M. C., Finkelstein, K. D. & Thorne, R. E. (2002). *Acta Cryst.* D**58**, 459–471.
Kriminski, S., Kazmierczak, M. & Thorne, R. E. (2003). *Acta Cryst.* D**59**, 697–708.
Kurinov, I. V. & Harrison, R. W. (1995). *Acta Cryst.* D**51**, 98–109.
Lu, Z. P. & Liu, C. T. (2003). *Phys. Rev. Lett.* **91**, 115505.
Mayer, E. (1985). *J. Appl. Phys.* **58**, 663–667.
Mazur, P. (1970). *Science*, **168**, 939-.
McFerrin, M. B. & Snell, E. H. (2002). *J. Appl. Cryst.* **35**, 538–545.
Peyridieu, J. F., Baudot, A., Boutron, P., Mazuer, J., Odin, J., Ray, A., Chapelier, E., Payen, E. & Descotes, J. L. (1996). *Cryobiology*, **33**, 436–446.
Pflugrath, J. W. (2004). *Methods*, **34**, 415–423.
Rodgers, D. W. (1994). *Cryocrystallogr. Struct.* **2**, 1135–1140.
Ryan, K. P. (1992). *Scanning Microsc.* **6**, 715–743.
Ryan, K. P., Bald, W. B., Neumann, K., Simonsberger, P., Purse, D. H. & Nicholson, D. N. (1990). *J. Microsc.* **158**, 365–378.
Sandalova, T., Schneider, G., Kack, H. & Lindqvist, Y. (1999). *Acta Cryst.* D**55**, 610–624.
Scheidig, A. J., Burmester, C. & Goody, R. S. (1999). *Structure*, **7**, 1311–1324.
Snell, E. H., Judge, R. A., Larson, M. & van der Woerd, M. J. (2002). *J. Synchrotron Rad.* **9**, 361–367.
Teng, T. Y. & Moffat, K. (1998). *J. Appl. Cryst.* **31**, 252–257.
Tilton, R. F., Dewan, J. C. & Petsko, G. A. (1992). *Biochemistry*, **31**, 2469–2481.
Walker, L. J., Moreno, P. O. & Hope, H. (1998). *J. Appl. Cryst.* **31**, 954–956.
Weik, M., Kryger, G., Schreurs, A. M. M., Bouma, B., Silman, I., Sussman, J. L., Gros, P. & Kroon, J. (2001). *Acta Cryst.* D**57**, 566–573.
Weik, M., Schreurs, A. M. M., Leiros, H. K. S., Zaccai, G., Ravelli, R. B. G. & Gros, P. (2005). *J. Synchrotron Rad.* **12**, 310–317.
Weik, M., Vernede, X., Royant, A. & Bourgeois, D. (2004). *Biophys. J.* **86**, 3176–3185.
Young, A. C. M., Tilton, R. F. & Dewan, J. C. (1994). *J. Mol. Biol.* **235**, 302–317.
Zeitler, E. (1982). *J. Ultrastruct. Res.* **81**, 397.